



ELSEVIER

Contents lists available at SciVerse ScienceDirect

European Polymer Journal

journal homepage: www.elsevier.com/locate/europolj

Macromolecular Nanotechnology

Comparison of filler percolation and mechanical properties in graphene and carbon nanotubes filled epoxy nanocomposites

M. Martin-Gallego*, M.M. Bernal, M. Hernandez, R. Verdejo, M.A. Lopez-Manchado*

Instituto de Ciencia y Tecnología de Polímeros, ICTP-CSIC, Juan de la Cierva 3, 28006 Madrid, Spain

ARTICLE INFO

Article history:

Received 26 October 2012

Received in revised form 6 February 2013

Accepted 20 February 2013

Available online xxxxx

Keywords:

Polymer nanocomposites

Graphene

Carbon nanotubes

Rheology

ABSTRACT

This paper compares the filler percolation network of multi-walled carbon nanotubes (MWCNTs) grown by chemical vapor deposition and thermally reduced functionalized graphene sheets (FGSs) in an epoxy resin. The filler network was evaluated by the plate-plate rheological response of un-cured dispersions and the electrical properties of cured materials. We found that FGS did not raise the viscosity of the system as much as MWCNT, maintaining the Newtonian behavior even at 1.5 wt.% FGS. MWCNT readily formed a filler network compared to FGS, evidenced by lower electrical and rheological percolation thresholds, presence of yield stress and higher storage modulus of the dispersions. On the other hand, the mechanical performance of the cured FGS nanocomposites outperformed the MWCNT, with enhancements of 50% and 15% of Young's modulus and strength, respectively. This combination of good processing properties with low viscosity and enhanced mechanical properties makes FGS great candidates to develop multifunctional polymer materials.

© 2013 Elsevier Ltd. All rights reserved.

1. Introduction

In the last decades, polymer nanocomposites with carbon based nanofillers have been widely studied in order to develop materials with multifunctional properties like high mechanical performance and heat dissipation, damage sensing [1–3], electrostatic discharge, large operating temperature range and chemical resistance among others [4]. Furthermore, in the last few years, researchers have made vast studies in performing multifunctional polymer nanocomposites based on carbon nanotubes (CNTs) and graphene sheets [5–8] due to the extraordinary intrinsic properties of these fillers.

Nanofiller morphology could greatly influence both processing and final properties of nanocomposites. Comparative studies of the final properties of sheet-like (graphene) and rod-like (CNTs) polymer nanocomposites

are starting to appear, due to the recent large availability of graphene. For example, Du et al. [9] comparatively studied the electrical properties of graphene and CNT high density polyethylene nanocomposites. They observed lower percolation thresholds and higher conductivities for the CNT nanocomposites. Meanwhile, graphene sheets nanocomposites show a better mechanical performance [10,11] which is attributed to the large specific area and planar geometry of the graphene and/or to a better mechanical interlocking of the nanofiller/matrix interface. A significant number of articles regarding the rheology of CNTs in polymers, especially epoxy resins, can be found in the literature [12–19]. However, to the best of our knowledge, no experimental works have already been completed comparing the rheological behavior and, hence, processing properties of graphene and CNTs polymer nanocomposites.

It is well known that the greatest enhancements on the properties of nanocomposites are reached when a network of the filler is formed within the polymer matrix. There are two main strategies to analyze filler networks when we

* Corresponding authors. Tel.: +34 912587424.

E-mail addresses: m.martingallego@ictp.csic.es (M. Martin-Gallego), lmanchado@ictp.csic.es (M.A. Lopez-Manchado).

use conductive particles. The first one is by analyzing the rheological response of the dispersion in the liquid state and the second one is by evaluating the electrical properties [15–18], in both cases the material presents a clear change of the variables involved in the analysis, either rheological or electrical studies, when we pass from a non-percolated system to a percolated one. It is worth mentioning that the rheology of the dispersions plays a key role from a processing point of view due to the big increments in the viscosity of the system when we add nanoparticles, favoring the presence of voids.

In this paper we evaluate the formation of filler networks for multi-walled carbon nanotubes (MWCNTs) and thermally reduced functionalized graphene sheets (FGSs) epoxy nanocomposites by means of their rheological behavior and electrical conductivity. Finally, we also tested their mechanical performance and concluded that FGS nanocomposites present a wider range of improvement than MWCNTs due to the lower viscosity of the initial dispersions and higher mechanical enhancement at low filler contents.

2. Experimental part

2.1. Materials

Diglycidyl ether of bisphenol-A epoxy resin (product number: 405493), and diethylene triamine curing agent (D93856) used in this study were purchased from Sigma-Aldrich, while multi-walled carbon nanotubes (MWCNTs) with an aspect ratio between 2500 and 3000 and a specific surface area of $50 \text{ m}^2/\text{g}$ [20,21] were synthesized in-house by a chemical vapor deposition technique [22]. Functionalized graphene sheets (FGSs) were also synthesized in-house by the rapid thermal expansion of graphite oxide (GO) at 1000°C under an inert atmosphere. This results in a high surface area carbon material consisting on wrinkled graphene layers with residual hydroxyl, carbonyl and epoxy groups. The atomic amount of oxygen atoms, estimated by XPS (data not shown) is 9.2%. GO was synthesized from natural graphite flakes obtained from Sigma-Aldrich (universal grade, purum powder $\leq 0.1 \text{ mm}$, 200 mesh, 99.9995%), according to the Brödie method. Full characterization of the functionalized graphene sheets used in this work is described elsewhere [23].

2.2. Characterization

FGS and MWCNTs were directly dispersed in the epoxy resin by means of Ultraturrax and sonication batch, a mixing procedure at 30,000 rpm for 10 min and 60 min in an ultrasonic bath at 60°C was carried out to reach a good dispersion of the carbon filler in the epoxy resin.

The rheological measurements were performed using a TA Instruments Advanced Rheometer AR1000. The geometry used was a stainless-steel parallel plate with a diameter of 25 mm. The gap was fixed to 0.25 mm and the measurements were recorded in frequency from 0.01 to 100 Hz at 21°C and at an amplitude of 1% in order to be within the linear viscoelastic range. The results are averaged over three different samples. The standard error for each set of samples was less than 1%.

The next protocol was followed to cure the formulations: the liquid formulations containing nanoparticles and epoxy resin were mixed with diethylene triamine in a stoichiometric ratio; the blends were degassed for 15 min in a vacuum chamber and casted in Teflon molds. Thermal treatments of 60 min at 70°C and 90 min at 130°C were applied to complete the curing reaction (DSC measurements were carried out to prove the material was completely cured). Electrical conductivity of the cured nanocomposites was determined on an ALPHA high-resolution dielectric analyzer (Novocontrol Technologies GmbH, Hundsangen, Germany) over a frequency range window of 10^{-1} – 10^7 Hz at room temperature. The cured films were held in the dielectric cell between two parallel gold-plated electrodes. The amplitude of the alternating current electric signal applied to the samples was 1 V.

The dispersion state of the nanoparticles was examined using transmission electron microscopy (TEM Leo 910 microscope at an acceleration voltage of 80 kV). Ultra-thin sections of the cured samples were prepared by cryo-ultramicrotomy at -140°C (Leica EM UC6).

Tensile tests were performed with dog-bone specimens using an Instron model 3366 tensile tester at a crosshead speed of 1 mm/min. The results are the average of at least five measurements.

3. Results and discussion

3.1. Rheological response (un-cured state)

The formation of filler networks in nanocomposites can be determined evaluating the rheological response in the melt state of the system. In the case of epoxy resins, the rheological measurements have to be performed before the curing reaction takes place.

Fig. 1a shows the variation of the complex viscosity versus frequency for studied systems. Epoxy resin clearly has a Newtonian flow behavior with the viscosity independent of the frequency. The addition of MWCNTs significantly alters the flow behavior of the epoxy dispersions. The viscosity gradually increases as the MWCNT content increases. This effect is particularly evident in the low frequency range and decreases with increasing frequency due to shear-thinning behavior. When the viscosity is plotted versus the torque applied (Fig. 1b) we can observe the presence of a yield stress for MWCNT dispersions because the viscosity tends asymptotically to infinite at a certain value of torque. Below that stress limit the material does not flow, showing a solid-like behavior. These changes in the rheological behavior are attributed to the formation of a nanotube network randomly dispersed. As high enough shear rates are applied, this network breaks down and CNTs can then align in the direction of the flow and/or dis-aggregate [24] causing the decrease in the viscosity. On the other hand, FGS does not change the Newtonian regime of the pristine epoxy resin, therefore, the effect of FGS concentration on the viscosity is much smaller compared with the viscosity enhancement produced by MWCNTs.

The increase in the viscosity as a function of MWCNT loading fraction and the change from Newtonian to

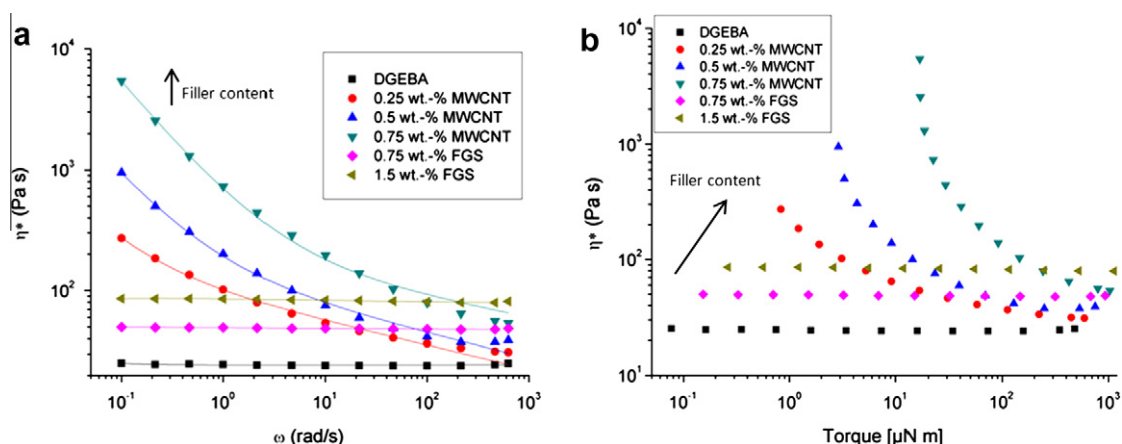


Fig. 1. Evolution of the complex viscosity of the epoxy/nanofiller dispersions: (a) versus frequency where the symbols correspond with the experimental result and the solid line with the Herschel–Bulkley model and (b) versus the torque.

shear-thinning response can be ascribed to the particle–particle and/or polymer–particle interactions. Poetschke et al. [25] found similar empirical results between CNTs and expanded graphite while Knauer et al. [26] performed simulations comparing the effect of nanoparticle shape, spherical, rod-like, and sheet-like nanoparticles on polymer nanocomposite rheology. They found the largest increase in viscosity for the rod-like nanoparticles and the least for the sheet-like. The authors explained this phenomenon based on the number of “bridging chains”, or polymer–particle interactions, present in the system. However, it has also been demonstrated that the destruction of a combined carbon nanotube/polymer network is feasible for polymers of high molecular weight [27] but is not contemplated for systems of low molecular weight. In our case, the system under study is a pre-polymer with a molecular weight of 337 g/mol, and, hence, it is assumed that a physical MWCNT network is the mechanism that takes place. Such consideration was proposed by Chapartegui et al. for CNT/epoxy dispersions [14]. Here, we observe that MWCNTs readily form a nanofiller network compared to FGS. This extended nanoparticle network is responsible for the increase in the viscosity and the change from Newtonian to shear-thinning response. Other experimental results with graphite oxide suspensions in PDMS corroborate this theory [28].

Several empirical equations have been proposed to describe the shear-thinning behavior of nanofiller dispersions. In our case the evolution of the frequency dependence of the viscosity is fitted by applying the Herschel–Bulkley model (Eq. (1)):

$$\eta^* = \frac{\tau_0}{\omega} + k\omega^{(n-1)} \quad (1)$$

where η^* is the complex viscosity, ω the angular frequency, τ_0 the yield stress, k the consistency index and n is the flow behavior index. When $n > 1$, the fluid exhibits a shear-thickening behavior; for $n = 1$ the fluid has a Newtonian behavior; when $n < 1$ the fluid shows shear-thinning behavior. The fitting parameters are summarized in Table 1 and the curves are represented with solid lines in Fig. 1a.

Table 1
Parameters of the Herschel–Bulkley fitting.

	τ_0 (Pa)	k (Pa s ⁿ)	n	R^2
DGEBA	≈0	24.4	1	0.97
0.25 wt.% MWCNT	13.5	88.2	0.8	0.99
0.5 wt.% MWCNT	75.7	116.9	0.8	0.99
0.75 wt.% MWCNT	510.6	191.3	0.8	0.99
0.75 wt.% FGS	≈0	49.3	1	0.96
1.5 wt.% FGS	≈0	85.6	1	0.99

This model has already been used to describe the non-linear viscoelastic behavior of CNTs dispersions [24,29–31].

We can observe a good correlation of the Herschel–Bulkley model with the experimental data, providing a good prediction of the rheological behavior of the filled epoxy dispersions. The decrease of the flow behavior index with the addition of MWCNTs means that the dispersion behaves like a shear thinning fluid. This theoretical model corroborates the tendency of the yield stress to increase with the amount of MWCNTs that is attributed to the nanofiller network which possesses certain strength by itself.

In the plot of the frequency sweep (Fig. 2), the storage modulus (G') of the neat epoxy resin follows a classical linear viscoelastic curve, this is called terminal or liquid-like behavior. In the case of the mixtures containing MWCNTs we can observe a plateau in the low frequency zone of the G' curves, termed as non-terminal or solid-like behavior. As the nanotube content increases the storage modulus also increases, becoming more independent of frequency and hence the plateau becomes larger. According to this idea and observing the curves, we are able to confirm that the rheological percolation thresholds are close to 0.25 wt.% and above 1.5 wt.% for MWCNT and FGS, respectively. These values agree with those found in the literature [14,32]. The G' values for the mixtures with MWCNTs are larger than those obtained with FGS which support our theory that the MWCNTs form a stronger and more interconnected network of particles. In addition, due to their planar geometry FGS could slip one from each other when

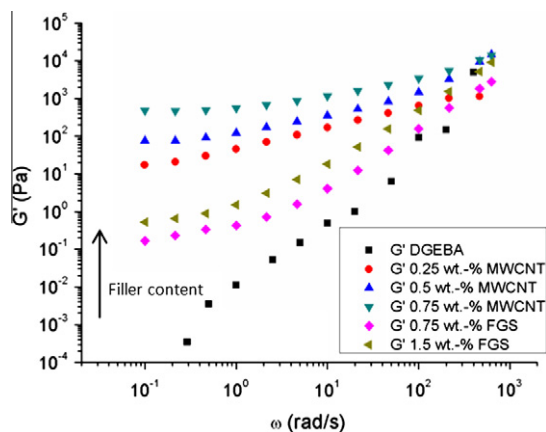


Fig. 2. Dynamic frequency sweeps for MWCNT/FGS dispersions.

the rotational force is applied to the system leading to lower storage moduli.

When we represent the storage and loss modulus together for the formulations with different contents of MWCNT (Fig. 3a) we can observe that at low frequency values, the G' became higher than the G'' at 0.5 and 0.75 wt.% of MWCNT. This also evidences of a solid-like behavior. The solid response characterized by $G' > G''$ started with the lowest concentration (0.25 wt.% of MWCNT) where $G' = G''$ at 0.1 rad/s, this fact tells us that the rheological percolation threshold is in the proximity of that concentration of filler. Comparing the effect of MWCNT and FGS at the same concentration (Fig. 3b), we clearly observe the solid-like response of the MWCNT characterized by $G' > G''$ at low frequencies while the FGS dispersion still presents a liquid-like behavior ($G'' > G'$). This liquid-like behavior is also observed at 1.5 wt.% of FGS supporting results obtained by other authors in similar systems [28].

If we consider the damping factor ($\tan \delta$) definition like the ratio between G''/G' we can represent it in a frequency sweep as in the Fig. 4. We are able to observe the presence of a maximum that becomes broader and appears at higher

frequencies when the nanoparticles are included. This peak in $\tan \delta$ is related to molecular motions in polymers and marks a certain limit in the mobility of polymer chains in a nanocomposite [33]. It is important to notice how the presence of MWCNTs largely reduces the value of $\tan \delta$ due to the increase in the elastic response discussed earlier.

From the figure 4, it is possible to define a characteristic time λ at which $\tan \delta$ maximum occurs ($\lambda = 1/\omega$). At a constant temperature, the chain mobility which requires times larger than λ implies that the terminal zone is hindered. On the other hand, motions involving times shorter than λ in the high frequency zone correspond to motions across entanglements and are not hindered by the presence of any of the nanoparticles. Thus, when the $\tan \delta$ peak appears at short times this means that the blocking effect of the particles is more effective and the mobility of polymer chains is more restricted. Looking at Table 2, the values of λ are notable shorter for MWCNTs than for FGS and the pristine epoxy resin. This feature is an indicative that FGS blocking effect in the un-cured resin is delayed compared to the MWCNT.

3.2. Electrical percolation (cured state)

The electrical percolation network of the cured samples is also analyzed. The AC electrical conductivity of the cured epoxy nanocomposites at different nanofiller contents measured at room temperature are depicted in Fig. 5.

We can observe how the filler network formed with MWCNT presents higher values of the electrical conductivity and lower electrical percolation threshold (lower than 0.25 wt.%) than FGS which percolates around 1.5 wt.%. This second strategy to evaluate filler networks shows the readily formation of the filler network with MWCNT. Nanocomposites with FGS not only percolate at higher filler contents, but also their conductivity is several orders of magnitude lower than MWCNT composites. This is due to the disturbance of the crystalline graphitic structure of the carbon nanofillers by the functionalization, reducing the number of π -electrons and generating more

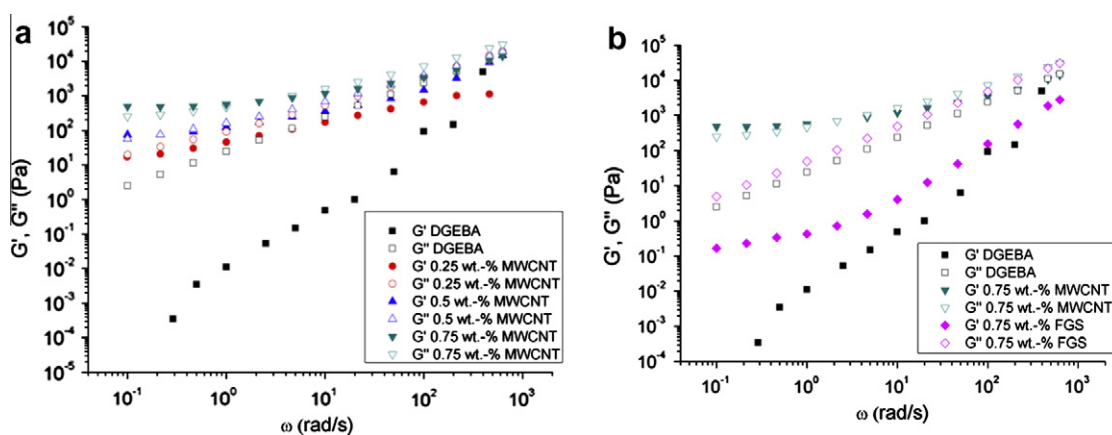


Fig. 3. Evolution of G' and G'' versus frequency at room temperature for the dispersions containing (a) MWCNT and (b) MWCNT and FGS at the same filler content.

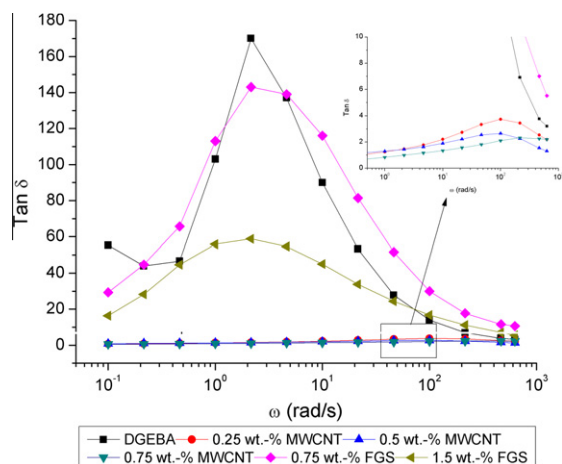


Fig. 4. Loss tangent as function of frequency for all the dispersions.

sp³-carbons which do not cause such high electronic transport as π -electrons [34]. Moreover, the macroscopic electrical behavior of the material is also influenced by tunneling conduction mechanisms and interparticle connections [35] which are less effective in the case of FGS.

3.3. Morphology (cured state)

We investigated the morphology and dispersion states of the cured samples with the highest amount of filler by TEM. Fig. 6a corresponds to the sample with 0.75 wt.% of MWCNT presenting a good dispersion state with isolated MWCNT. It is possible to see some overlapping connections among them (marked with arrows) which are responsible for the highly effective electronic transport through their crystalline structure.

Fig. 6b shows the morphology of the 1.5 wt.% FGS nanocomposite where it is possible to observe the wrinkled shape of the sheets and their more stacked structured with different type connections such as plane-to-plane, edge-to-plane and edge-to-edge which are not as electrically efficient as the overlapping of CNTs [9] but do not rise the viscosity as much as the CNT network.

3.4. Mechanical properties (cured state)

Tensile tests were performed in all the compositions in order to obtain the stiffness, strength and elongation of the composites. The results are summarized in Table 3. It can be clearly noted how Young's modulus increases with the filler content for both types of reinforcements. We could only reach 0.75 wt.% of MWCNT due to the extremely high viscosity of the system giving an enhancement of 38% in Young's modulus and 20% in the final strength while the fi-

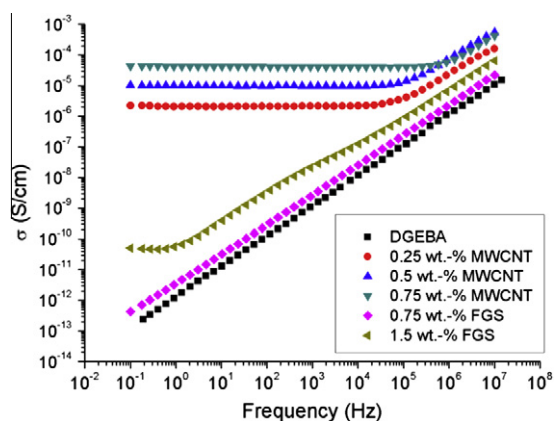


Fig. 5. AC electrical conductivity of the cured samples.

nal elongation is reduced. The explanation to this stiffening effect without reducing the strength of the material is attributed to an appropriate impregnation with the matrix and good adhesion at the filler/matrix interphase [36].

On the other hand, the lower viscosity of the FGS dispersions allows us to double the maximum MWCNT concentration. The improvement obtained with 1.5 wt.% of FGS is higher than 50% and 15% for Young's modulus and final strength, respectively. This means that with FGS we are able to use a broader range of concentrations leading to better improvements of the final properties compared to CNT composites.

Fig. 7 shows a comparison of the tensile curves for the neat epoxy resin and the nanocomposites containing 0.5 wt.% of MWCNT, and FGS. We observed that the FGS outperform the MWCNTs nanocomposites. This could be the result of the morphological differences and/or the presence of functional groups. To elucidate these effects, we oxidized the MWCNTs (o-MWCNT) to bear similar functional groups than the FGS through a very well-known acid treatment with a mixture of H₂SO₄/HNO₃ [22,37]. We can observe that even though the o-MWCNT possesses lower aspect ratio [38], the final properties of their composites exceed the performance of the un-treated nanotubes due to their more affective wettability and interfacial adhesion produced by the chemical bonding of the functional groups with the epoxy matrix and the hardener [39]. FGS nanocomposites shows the most outstanding mechanical performance as previously reported [10,11]. This fact can be attributed to both effects, the functionalization and the planar geometry, predominantly to its morphology because the small thickness of the sheets with a much wrinkled topology at the nanoscale results in a better mechanical interlocking with the polymer chains and a more impeded crack propagation [40].

Table 2

Values of λ for all the dispersions.

	DGEBA	0.25 wt.% MWCNT	0.5 wt.% MWCNT	0.75 wt.% MWCNT	0.75 wt.% FGS	1.5 wt.% FGS
λ (s)	4.7×10^{-1}	10^{-2}	10^{-2}	4.7×10^{-3}	4.7×10^{-1}	4.7×10^{-1}

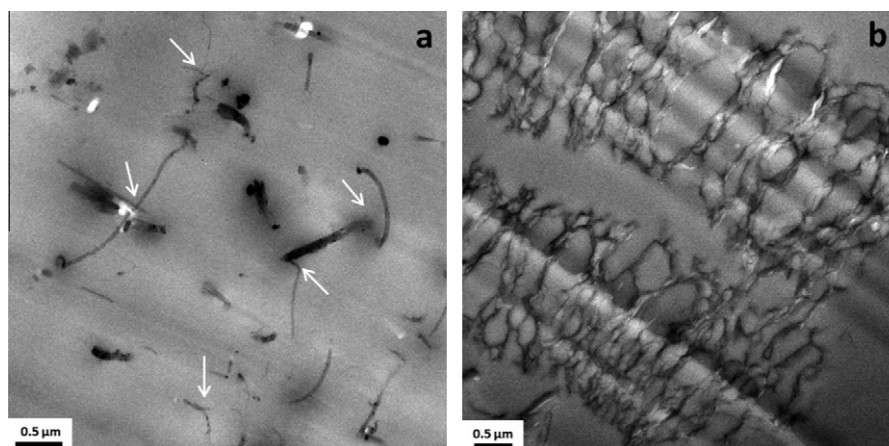


Fig. 6. TEM images of the 0.75 wt.% MWCNT and 1.5 wt.% FGS nanocomposites.

Table 3

Mechanical properties of the reinforced nanocomposites.

	E (MPa)	σ (MPa)	ε (%)
DGEBA	1631 ± 37	58.9 ± 3.5	5.9 ± 0.5
0.25 wt.% MWCNT	1954 ± 97	68.4 ± 3.1	5.4 ± 0.7
0.5 wt.% MWCNT	2005 ± 32	69.1 ± 6.8	4.8 ± 0.7
0.75 wt.% MWCNT	2267 ± 21	72.1 ± 3.6	4.9 ± 0.6
0.5 wt.% o-MWCNT	2039 ± 51	75.4 ± 2.0	5.7 ± 0.4
0.25 wt.% FGS	2163 ± 72	65.2 ± 4.0	4.3 ± 0.3
0.5 wt.% FGS	2296 ± 55	64.4 ± 6.6	3.8 ± 0.7
0.75 wt.% FGS	2393 ± 62	68.1 ± 7.6	3.7 ± 0.6
1.5 wt.% FGS	2466 ± 34	68.5 ± 8.3	3.7 ± 0.8

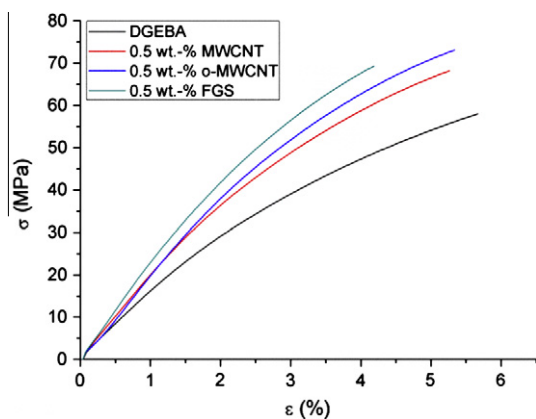


Fig. 7. Stress–strain curves for the neat resin and nanocomposites containing 0.5 wt.% of MWCNT, o-MWCNT and FGS.

4. Conclusions

We studied the percolation network of MWCNT and FGS epoxy nanocomposites through the rheology behavior of the dispersions and the final electrical properties of the nanocomposites. MWCNTs with a rod-like geometry and a very high aspect ratio readily form the filler network. A lower rheological and electrical percolation threshold for MWCNTs is observed. MWCNTs change the rheological

behavior from a Newtonian fluid to a shear-thinning response while the planar structure and functional groups on the FGS do not raise the viscosity of the dispersions even at high concentrations. This low viscosity plays a key role in their processing which allows us to introduce higher contents of FGS.

The tensile tests performed on the cured samples revealed notable enhancements in the elastic moduli and final strength of the composites, especially in the case of the nanocomposites containing FGS. This combination of good processing properties with low viscosities and enhanced final mechanical properties makes FGS great candidates to develop multifunctional polymer materials.

Acknowledgments

The work was supported by the Spanish Ministry of Science and Innovation (MICINN) under project MAT 2010-18749. All the authors gratefully acknowledge Dr. Fangfang Tao for her help with the rheological measurements. MMG and MMB also thank the JAE-Pre grant and FPI programs from the CSIC and MICINN, respectively.

References

- [1] Thostenson E, Chou T-W. Carbon nanotube networks: sensing of distributed strain and damage for life prediction and self healing. *Adv Mater* 2006;18(21):2837.
- [2] Monti M, Natali M, Petrucci R, Kenny JM, Torre L. Impact damage sensing in glass fiber reinforced composites based on carbon nanotubes by electrical resistance measurements. *J Appl Polym Sci* 2011;122(4):2829–36.
- [3] Monti M, Natali M, Petrucci R, Kenny JM, Torre L. Carbon nanofibers for strain and impact damage sensing in glass fiber reinforced composites based on an unsaturated polyester resin. *Polym Compos* 2011;32(5):766–75.
- [4] Leng J, Lau AKT. Multifunctional polymer nanocomposites. Boca Raton: CRC Press; 2011.
- [5] Chou T-W, Gao L, Thostenson E, Zhang Z, Byun J-H. An assessment of the science and technology of carbon nanotube-based fibers and composites. *Compos Sci Technol* 2010;70(1):1–19.
- [6] Verdejo R, Bernal MM, Romasanta L, Lopez Manchado M. Graphene filled polymer nanocomposites. *J Mater Chem* 2011;21(10):3301–10.
- [7] Terrones M, Martin O, Gonzalez M, Pozuelo J, Serrano B. Interphases in graphene polymer-based nanocomposites: achievements and challenges. *Adv Mater* 2011;23(44):5302–10.

- [8] Young R, Kinloch I, Gong L, Novoselov K. The mechanics of graphene nanocomposites: a review. *Compos Sci Technol* 2012;72(12):1459–76.
- [9] Du J, Zhao L, Zeng Y, Zhang L, Li F. Comparison of electrical properties between multi-walled carbon nanotube and graphene nanosheet/high density polyethylene composites with a segregated network structure. *Carbon* 2011;49(4):1094–100.
- [10] Rafiee M, Rafiee J, Wang Z, Song H, Yu Z-Z. Enhanced mechanical properties of nanocomposites at low graphene content. *ACS Nano* 2009;3(12):3884–90.
- [11] Martín-Gallego M, Hernandez M, Lorenzo V, Verdejo R, Lopez-Manchado MA. Cationic photocured epoxy nanocomposites filled with different carbon fillers. *Polymer* 2012;53(9):1831–8.
- [12] McClory C, McNally T, Baxendale M, Pötschke P, Blau W, Ruether M. Electrical and rheological percolation of PMMA/MWCNT nanocomposites as a function of CNT geometry and functionality. *Eur Polym J* 2010;46(5):854–68.
- [13] Yokozeki T, Carolin Schulz S, Buschhorn ST, Schulte K. Investigation of shear thinning behavior and microstructures of MWCNT/epoxy and CNF/epoxy suspensions under steady shear conditions. *Eur Polym J* 2012;48(6):1042–9.
- [14] Chapartegui M, Markaide N, Florez S, Elizetxea C, Fernandez M. Specific rheological and electrical features of carbon nanotube dispersions in an epoxy matrix. *Compos Sci Technol* 2010;70(5):879–84.
- [15] Schulz SC, Faiella G, Buschhorn ST, Prado LASA, Giordano M, Schulte K, et al. Combined electrical and rheological properties of shear induced multiwall carbon nanotube agglomerates in epoxy suspensions. *Eur Polym J* 2011;47(11):2069–77.
- [16] Schulz S, Schlutter J, Bauhofer W. Influence of initial high shearing on electrical and rheological properties and formation of percolating agglomerates for MWCNT/epoxy suspensions. *Macromol Mater Eng* 2010;295(7):613–7.
- [17] Bauhofer W, Schulz SC, Eken AE, Skipa T, Lellinger D, Alig I, et al. Shear-controlled electrical conductivity of carbon nanotubes networks suspended in low and high molecular weight liquids. *Polymer* 2010;51(22):5024–7.
- [18] Song YS, Youn JR. Influence of dispersion states of carbon nanotubes on physical properties of epoxy nanocomposites. *Carbon* 2005;43(7):1378–85.
- [19] Abdalla M, Dean D, Adibempe D, Nyairo E, Robinson P, Thompson G. The effect of interfacial chemistry on molecular mobility and morphology of multiwalled carbon nanotubes epoxy nanocomposite. *Polymer* 2007;48(19):5662–70.
- [20] Peigney A, Laurent C, Flahaut E, Bacsa RR, Rousset A. Specific surface area of carbon nanotubes and bundles of carbon nanotubes. *Carbon* 2001;39(4):507–14.
- [21] Singh C, Shaffer MS, Windle AH. Production of controlled architectures of aligned carbon nanotubes by an injection chemical vapour deposition method. *Carbon* 2003;41(2):359–68.
- [22] Verdejo R, Lamoriniere S, Cottam B, Bismarck A, Shaffer M. Removal of oxidation debris from multi-walled carbon nanotubes. *Chem Commun* 2007;5:513–5.
- [23] Verdejo R, Barroso Bujans F, Rodriguez Perez M, de Saja J, Lopez Manchado M. Functionalized graphene sheet filled silicone foam nanocomposites. *J Mater Chem* 2008;18(19):2221–6.
- [24] Xia H, Song M. Preparation and characterization of polyurethane-carbon nanotube composites. *Soft Matter* 2005;1(5):386–94.
- [25] Poetschke P, Abdel Goad M, Pegel S, Jehnichen D, Mark J. Comparisons among electrical and rheological properties of melt-mixed composites containing various carbon nanostructures. *J Macromol Sci, Pure Appl Chem* 2010;47(1):12–9.
- [26] Knauert S, Douglas J, Starr F. The effect of nanoparticle shape on polymer-nanocomposite rheology and tensile strength. *J Polym Sci, Part B: Polym Phys* 2007;45(14):1882–97.
- [27] Alig I, Skipa T, Lellinger D, Poetschke P. Destruction and formation of a carbon nanotube network in polymer melts: rheology and conductivity spectroscopy. *Polymer* 2008;49(16):3524–32.
- [28] Guimont A, Beyou E, Martin G, Sonntag P, Cassagnau P. Viscoelasticity of graphite oxide-based suspensions in PDMS. *Macromolecules* 2011;44(10):3893–900.
- [29] Bernal MM, Verdejo R. In situ foaming evolution of flexible polyurethane foam nanocomposites. *Macromol Chem Phys* 2011;212(9):971–9.
- [30] Tiwari M, Bazilevsky A, Yarin A, Megaridis C. Elongational and shear rheology of carbon nanotube suspensions. *Rheol Acta* 2009;48(6):597–609.
- [31] Kinloch IA, Roberts SA, Windle AH. A rheological study of concentrated aqueous nanotube dispersions. *Polymer* 2002;43(26):7483–91.
- [32] Kim H, Macosko C. Processing–property relationships of polycarbonate/graphene composites. *Polymer* 2009;50(15):3797–809.
- [33] Fernandez I, Santamaria A, Munoz M, Castell P. A rheological analysis of interactions in phenoxy/organoclay nanocomposites. *Eur Polym J* 2007;43(8):3171–6.
- [34] Gojny FH, Wichmann MHG, Fiedler B, Kinloch IA, Bauhofer W. Evaluation and identification of electrical and thermal conduction mechanisms in carbon nanotube/epoxy composites. *Polymer* 2006;47(6):2036–45.
- [35] Simmons JG. Generalized formula for the electric tunnel effect between similar electrodes separated by a thin insulating film. *J Appl Phys* 1963;34(6):1793–803.
- [36] Gojny FH, Wichmann MHG, Köpke U, Fiedler B, Schulte K. Carbon nanotube-reinforced epoxy-composites: enhanced stiffness and fracture toughness at low nanotube content. *Compos Sci Technol* 2004;64(15):2363–71.
- [37] Verdejo R, Staempfli R, Alvarez Lainez M, Mourad S, Rodriguez-Perez MA. Enhanced acoustic damping in flexible polyurethane foams filled with carbon nanotubes. *Compos Sci Technol* 2009;69(10):1564–9.
- [38] Rosca ID, Watari F, Uo M, Akaska T. Oxidation of multiwalled carbon nanotubes by nitric acid. *Carbon* 2005;43(15):3124–31.
- [39] Gojny FH, Wichmann MHG, Fiedler B, Schulte K. Influence of different carbon nanotubes on the mechanical properties of epoxy matrix composites – a comparative study. *Compos Sci Technol* 2005;65(15–16):2300–13.
- [40] Ramanathan T, Abdala AA, Stankovich S, Dikin DA, Herrera Alonso M. Functionalized graphene sheets for polymer nanocomposites. *Nat Nanotechnol* 2008;3(6):327–31.